Response to the open reviewer,

We sincerely appreciate your expert insight and thoughtful suggestions. Your comments can be broadly categorized into the following points, and we will address each of them accordingly.

1. Overview of surface reference techniques in previous studies
2. Concerns regarding Doppler velocity averaging and potential aliasing
3. Assumptions about zero surface velocity and consideration of NUBF effects
4. Validity of applying corrections over land and associated errors
5. Consistency of spatial and temporal scales
6. Treatment of differences between ascending and descending nodes
7. Clarification regarding the use of the digital elevation model (DEM)
8. Handling of uncertainties over Antarctic sea ice

Response to Comments 1–3

Thank you for your detailed and thoughtful comments.

With regard to Comments 1–3, we would like to clarify that these points fall outside the scope of the present study.

The primary objective of this manuscript is the analysis of cloud microphysical properties using Doppler velocity observations, rather than a methodological assessment of the antenna mispointing error correction itself. In this study, we use the JAXA Level 2 Doppler velocity product, in which the antenna mispointing correction has already been applied. A comprehensive description, validation, and discussion of the correction methodology—including surface reference techniques, Doppler velocity averaging and aliasing, and assumptions regarding zero surface velocity and NUBF effects—are currently being prepared in a dedicated manuscript of ATBD led by Dr. Shunsuke Aoki as part of the JAXA Level 2 product development.

Including a detailed treatment of these topics in the present manuscript would go beyond its intended scope and detract from its main focus on cloud microphysics. Therefore, we do not address Comments 1–3 within this paper, and we respectfully defer these aspects to the forthcoming JAXA-led publication, where they can be discussed in a technically rigorous and comprehensive manner.

Response to Comments 4; 5; 6; and 8.

We agree that the correction over land surfaces can introduce systematic errors. We have therefore revised the land mask based on surface heterogeneity and seasonality, and re-performed the analysis accordingly. The reliability criteria about the antenna mispointing error correction are described in detail in Appendix B.

First, following the antenna mispointing error correction performed by Dr. Aoki (JAXA), which uses a 100 km moving average, we decided to evaluate the data reliability for each $1° \times 1°$ pixel. This modification addresses Comment 5 in the introductory remarks.

Next, the data reliability assessment is now conducted separately for the Ascending Node and Descending Node. This modification addresses Comment 6 in the introductory remarks.

The specific procedure for the data reliability evaluation is described below.

First, based on the NCEP-FNL reanalysis data used in this study, we generated a sea-ice coverage map for the analysis period. Any pixel that is even partially covered by sea ice was excluded from the analysis. This modification addresses Comment 8.

This approach follows the analysis shown in Figure 3 of Treserras et al. (2025). In our previous analysis, we also confirmed that the σ_{fit} of the surface Doppler velocity is significantly larger over sea ice. The sea-ice map used for the filtering is shown below.
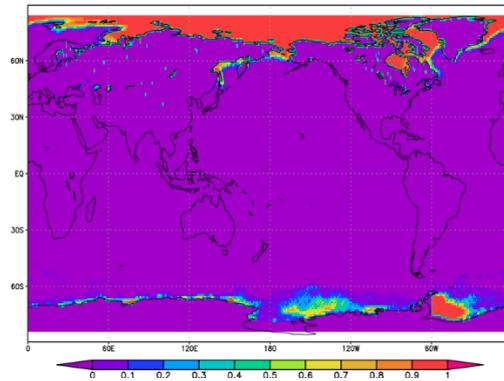

Figure OR1. Global distribution of sea-ice concentration from NCEP-FNL product (ICEC). The values represent the three-month mean averaged over January-March 2025.
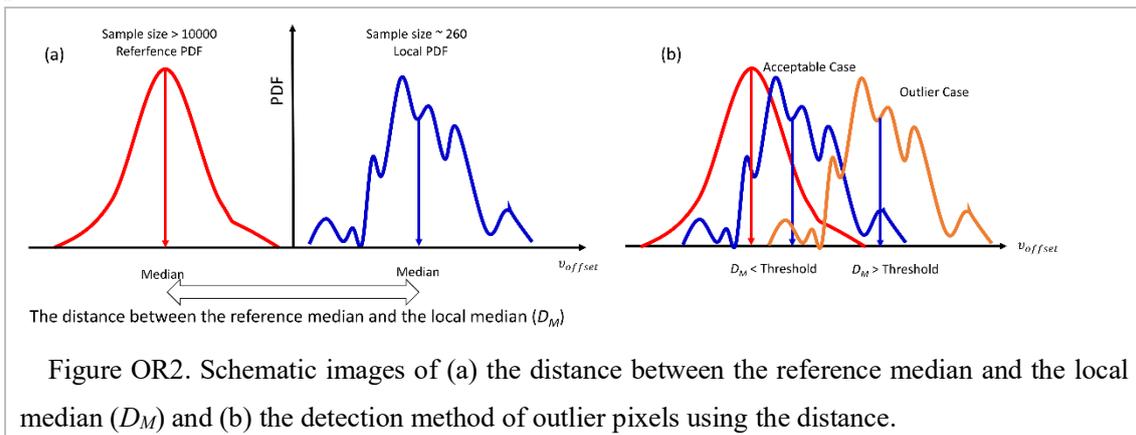
Next, we describe the method used to detect pixels with low reliability. First, over ocean regions not covered by sea ice, a probability density function (PDF) of the Antenna Mispointing Error Correction value (v_{offset}) is constructed at $1°$ latitude intervals. This PDF is referred to as the reference PDF.

For each $1° \times 1°$ pixel, a separate PDF of the Antenna Mispointing Error Correction values is also generated, which we refer to as the local PDF. If the distance between the local PDF and the reference PDF is sufficiently large, the corresponding pixel is regarded as having low reliability and is excluded from the analysis. A schematic illustration of this procedure is shown in Figure OR2. Hereafter, the distance between the reference median and the local median is referred to as D_M.

Since the reliability assessment is performed for each $1° \times 1°$ pixel, the number of observational samples obtained for each pixel during the three-month analysis period is approximately 260 on

average. When analyzing v_{offset} with 1 cm s^{-1} bins, a smooth PDF typically requires 1500–3000 samples. Therefore, applying parametric statistical measures, such as the standard deviation, is not appropriate for evaluating the distance between the reference PDF and the local PDF.

Instead, we adopt a non-parametric analysis based on percentiles. Specifically, if the 50th percentile (median) of v_{offset} in the local PDF lies outside the 1σ-equivalent percentile range of the reference PDF (i.e., v_{offset} < 16th percentile or v_{offset} > 84th percentile), the pixel is classified as a 1σ outlier. Similarly, we also evaluate 2σ outliers, defined as pixels satisfying v_{offset} < 2.5th percentile or v_{offset} > 97.5th percentile.

Figure OR2. Schematic images of (a) the distance between the reference median and the local median (D_M) and (b) the detection method of outlier pixels using the distance.
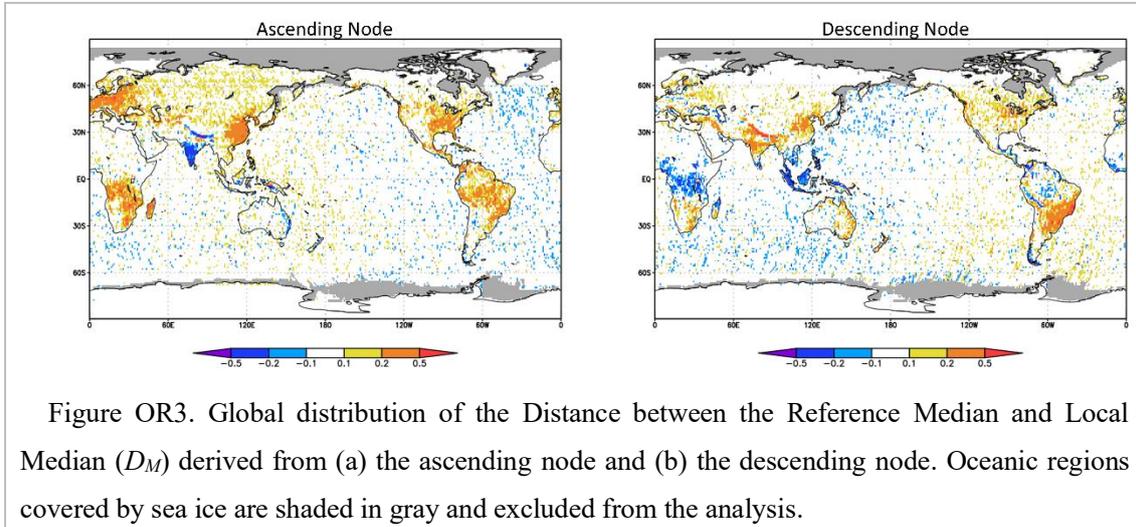
First, we describe the construction of the reference PDF. The reference PDF must be derived from a sufficiently large number of samples representing reliable surface conditions. According to Figure 3 of Treserras et al. (2025), measurements over the Antarctic continent with sufficient snow cover and over Greenland also exhibit high reliability.

Therefore, south of 68°S, the number of ocean samples becomes very small (fewer than 10,000 samples), and thus values over the Antarctic continent were used instead. In contrast, during the Northern Hemisphere winter, the number of samples north of 76°N falls below 10,000, and therefore a reference PDF was not constructed from ocean data in this region. However, since Greenland has a complex coastline, it is difficult to automatically remove locations with potentially low reliability associated with surface topography. For this reason, to ensure the robustness of the analysis, regions north of 76°N were excluded from the analysis in this study.

The horizontal distribution of the Distance between the Reference Median and Local Median (D_M) is shown below. A larger D_M indicates lower reliability of the Antenna Mispointing Error Correction. First, although regions with large D_M appear in similar locations for the Ascending Node and Descending Node, the magnitude of D_M differs slightly between them. This result is consistent with the reviewer's comment.
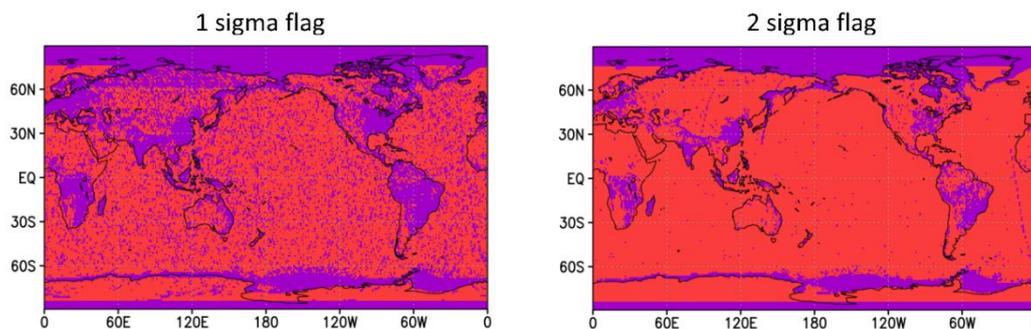
Due to the limited number of samples, a small number of pixels with relatively large D_M values are

scattered even over ocean regions. However, in general, the results indicate that low reliability mainly occurs over land under specific surface conditions. These low-reliability pixels largely coincide with the regions excluded in Figure 10d of the preprint version of this study. However, by performing the analysis at the 1° × 1° pixel scale, the present method allows us to more precisely identify the regions that should be excluded.

Figure OR3. Global distribution of the Distance between the Reference Median and Local Median (D_M) derived from (a) the ascending node and (b) the descending node. Oceanic regions covered by sea ice are shaded in gray and excluded from the analysis.

Finally, the global distributions of 1σ outlier pixels and 2σ outlier pixels are shown in Figure OR4. When 2σ outliers are excluded, almost no oceanic pixels are removed, while pixels with large deviations over land are selectively filtered out. This result indicates that under certain land surface conditions, the antenna mispointing error correction becomes unrealistically large, reaching values that rarely occur over the ocean (i.e., below the 2.5th percentile or above the 97.5th percentile of the reference distribution).

In contrast, when 1σ outliers are excluded, most land pixels are removed from the analysis. This indicates that even regions with relatively small deviations, as shown in Figure OR3, are excluded

Figure OR4. Global distribution of 1σ outlier pixels and 2σ outlier pixels determined from the percentile deviation of the local median relative to the reference PDF.

under the 1σ criterion. This approach increases the reliability of the retained dataset although it substantially reduces the number of available samples and some oceanic pixels that are likely reliable

are also removed due to the limited sample size within each 1° × 1° pixel. Therefore, this filter is applied to pixels only over land. Finally, we chose the threshold of 1σ to exclude outliers after checking the spatial distribution of σ_{fit} for Figure 10.

This percentile-based approach allows robust reliability assessment even when the local PDFs are noisy due to the limited number of samples within each 1° × 1° pixel. This approach enables a two-order-of-magnitude improvement in spatial resolution compared with the initial 10° × 10° reliability assessment. This framework allows systematic identification of unreliable pixels while preserving reliable oceanic observations.

In Fig. 10 of the manuscript, a large number of samples are required to estimate σ_fit; therefore, the analysis is performed using 10° × 10° grid cells. To illustrate the sampling statistics after applying the filtering procedure, the number of samples within each 10° × 10° grid cell is shown in Fig. OR5.

For both the ascending and descending nodes, it can be seen that the sample numbers become extremely low in regions where pixels with low data reliability have been removed. When the number of samples falls below 3000, the resulting probability density function (PDF) becomes noisy, making it difficult to estimate σ_fit using the parametric analysis. Therefore, such pixels are excluded from the analysis.

Although the final set of excluded pixels is largely similar to that in the original manuscript, the approach used to identify unreliable pixels differs in the revised analysis. These analyses are included in the Appendix, and they are referenced in the main text immediately after Figure 8.
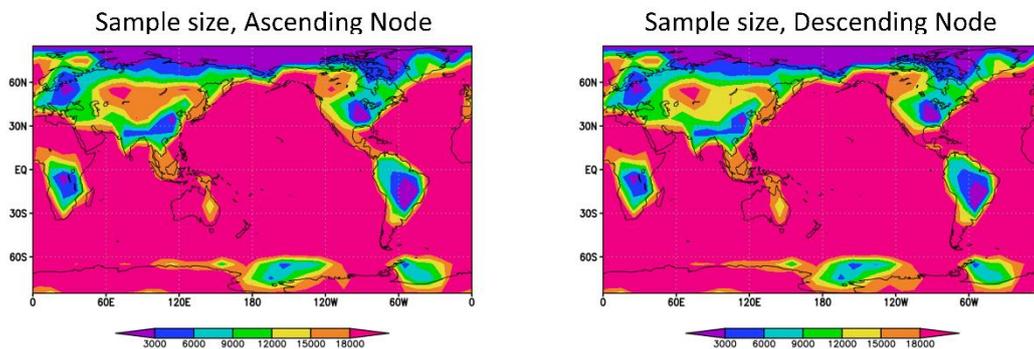

Figure OR5. Global distribution of the number of samples within each 10° × 10° grid cell. A 1σ outlier filter is applied over land, and regions covered by sea ice are excluded.

Response to comment 7. Use of DEM

The description in the original manuscript was not sufficiently clear, which may have led to confusion regarding the use of the DEM. This issue mainly arose from differences in the specifications

between the CPR_ECO Level 1 and Level 2 products, which we clarify here.

As the reviewer correctly noted, the surface height reference used in the Antenna Mispointing Error Correction is determined solely from the maximum radar echo intensity. In contrast, the Level 2 product includes a ground clutter flag, where the surface elevation derived from a Digital Elevation Model (DEM) is used to determine the distance from the surface more accurately, without being constrained by the radar range bin.

This approach is necessary because surface reflections in radar echoes can be extremely strong and may become saturated. In particular, when liquid water clouds are present near the surface, it becomes difficult to determine the surface height accurately using only the radar echo signal.

Based on this clarification, and because most of the reliability evaluation has now been moved to the Appendix, the corresponding description in the manuscript has been removed.

We thank the reviewer for pointing out this important issue, which helped us clarify the description in the manuscript.